



This document is a postprint version of an article published in Food Chemistry © Elsevier after peer review. To access the final edited and published work see <https://doi.org/10.1016/j.foodchem.2020.128891>

Document downloaded from:



1 **MICROANALYTICAL FLOW SYSTEM FOR THE**
2 **SIMULTANEOUS DETERMINATION OF ACETIC ACID AND**
3 **FREE SULFUR DIOXIDE IN WINES**

4 **Pablo Giménez-Gómez^{*a}, Manuel Gutiérrez-Capitán^a, Juan Manuel Ríos^a, Fina**
5 **Capdevila^b, Anna Puig-Pujol^b, and Cecilia Jiménez-Jorquera^{*a}**

6 ^a *Instituto de Microelectrónica de Barcelona (IMB-CNM), CSIC, Campus UAB, 08193*
7 *Bellaterra, Spain*

8 ^b *Institut Català de la Vinya i el Vi (IRTA-INCAVI), Plaça Àgora 2, 08720 Vilafranca*
9 *del Penedès, Spain*

10 * *Corresponding authors: Pablo Giménez-Gómez (e-mail: pablo.gimenez@csic.es) and*
11 *Cecilia Jiménez-Jorquera (e-mail: cecilia.jimenez@csic.es)*

12
13
14
15
16
17
18
19
20

21 **Highlights**

- 22 • An accurate and interference-free system based on a pH sensor and a gas-
23 diffusion membrane for the determination of acetic acid and free SO₂.
- 24 • A microanalytical portable flow system for the on-site control of wine aging.
- 25 • An automated compact system easy to install in ageing barrels.

26 **Abstract**

27 Free sulfur dioxide and volatile acidity are parameters related to the quality of
28 wines. Traditional methods for their determination are tedious, time consuming and
29 require analysis in decentralized laboratories, therefore corrective actions cannot be
30 applied on time. This may be more complex in aging wine cellars, where hundreds of
31 individual barrels containing almost finished wines should be monitored. To achieve
32 this aim, a portable microanalytical flow system for the simultaneous detection of free
33 SO₂ and acetic acid during the ageing of wines is proposed in this work. The
34 miniaturized system is based on the use of a gas-diffusion membrane and a pH-ISFET,
35 and can be easily installed in barrels. The system was optimized in the range of 5-60 mg
36 L⁻¹ and 0.15-1.40 g L⁻¹ for SO₂ and acetic acid, respectively. It was validated with
37 different sets of wine samples by comparing the results with standard methods,
38 demonstrating a good agreement between methods.

39 **Keywords:** miniaturized analytical flow-system; permeable gas-diffusion membrane;
40 pH-ISFET; monitoring of acetic acid and free sulfur dioxide; wine samples

41 **1. Introduction**

42 Volatile acidity and sulfur dioxide (SO₂) are two important parameters related to the
43 quality of the wine measured during the winemaking process (Bakker, Bridle,

44 Bellworthy, Garcia-Viguera, Reader & Watkins, 1998, Ribereau-Gayon, Dubourdieu,
45 Donèche, & Lonvaud, 2006a). An excess of volatile acidity is mainly related to a high
46 concentration of acetic acid, which can be produced in small concentration at the
47 beginning of alcoholic fermentation (AF). In addition, during the malolactic
48 fermentation (MLF) there is a slight increase of volatile acidity due to the metabolism
49 of some heterofermentative lactic acid bacteria strains and the breakdown of citric acid
50 and tartaric acid. Wine naturally has a volatile acidity of 0.15-0.70 g L⁻¹, expressed as
51 acetic acid. This value tends to increase slightly during aging due to the bacterial
52 activity. Acetic acid is not easily detectable for humans in wine if the concentration is
53 below 0.7-0.8 g L⁻¹. Above this value, the smell becomes acid and the flavor
54 deteriorates, becoming harsh and bitter on the finish. The maximum level of acetic acid
55 is fixed in the European Community by the International Organization of Vine and
56 Wine (OIV). This value varies depending on the wine class, 1.2 g L⁻¹ for most of wines,
57 although some old wines can exceed this limit because they are subjected to a particular
58 legislation (OIV, 2017).

59 Regarding sulfur dioxide, it is used to prevent the microbial spoilage, the oxidation
60 and the color changes of wine due to undesirable reactions (Fazio & Warner, 1990).
61 Nevertheless, the control of the SO₂ concentration in wine is essential to avoid
62 associated negative effects in the health of allergic consumers (e.g., breathing difficulty,
63 migraine or gastrointestinal disorder) (Adams, 1997). Moreover, disagreeable odor and
64 bad taste of wines can be caused if the SO₂ concentration exceeds a set value fixed by
65 the OIV in Europe (150 mg L⁻¹ and 400 mg L⁻¹ for red wines and sweet white wines,
66 respectively).

67 Sulfur dioxide can be found in wine in two forms: free and bound (Eschenbruch,
68 1974). Free sulfur dioxide is the most active form for protecting wine against spoilage

69 and oxidation. Therefore, by controlling the level of free sulfur dioxide, winemakers
70 promote the bacterial stability to guarantee the quality of the product (Ribereau-Gayon,
71 Dubourdieu, Donèche & Lonvaud, 2006a).

72 There is an important interdependence of these two parameters (acetic acid and free
73 sulfur dioxide) during the aging process of red wines in oak barrels. The aging process
74 enables the extraction of wood flavors, aromas and the production of phenolic
75 components that influence astringency and phenolic polymerization and, overall, this
76 process allows the organoleptic improvement of wines (Ribéreau-Gayon, Glories,
77 Maujean & Dubourdieu, 2006b). But throughout this aging period, there is a continuous
78 need of microbial control carried out by the addition of free sulfur dioxide in wine. The
79 prevention of unwanted yeast and bacterial activity (i.e. *Brettanomyces*, *Pediococcus*,
80 *Lactobacillus*, *Gluconobacter* and *Acetobacter*), that could cause an increase of acetic
81 acid in wine, is carried out by maintaining appropriate levels of molecular SO₂. The
82 molecular form corresponds to the undissociated form of the free SO₂ and its
83 concentration depends on the total concentration and the pH of the wine. It is
84 recommended to maintain a free SO₂ level of 20 – 40 mg L⁻¹ (Morata, 2019). For that
85 reason, it is important to check regularly both, acetic acid and free SO₂, along ageing in
86 barrels to avoid loss of organoleptic quality of wines.

87 Analytical methods used for free sulfur dioxide detection and defined by the OIV in
88 Europe are the Paul's method (OIV, 2009a), the Ripper's method (OIV, 2009b) and the
89 Beech and Thomas method (OIV, 2009c). Regarding the acetic acid, the steam
90 distillation/titration method (OIV, 2015) and the enzymatic method through automated
91 colorimetric analyzers (OIV, 2010) are used. These methods have limitations like low
92 accuracy for colored samples (i.e. red wines), they are time-consuming, and have to be
93 carried out in specialized laboratories by highly skilled personnel. Besides, the

94 enzymatic methods for acetic acid detection are not automated. Therefore, continuous
95 monitoring of these parameters in the ageing barrels is not available. Other alternative
96 methods described in the literature with more compact and simple equipment are those
97 using electrochemical biosensors (Adelaju & Hussain, 2016, Li, et al., 2019, Sroysee,
98 Ponlakheth, Chairam, Jarujamrus & Amatatongcha, 2016). However, they have problems
99 of biofouling and they are affected by some interferences, so their implementation in
100 portable systems for long-term monitoring is limited. Colorimetric methods combining
101 gas-diffusion systems for avoiding the interferences of the sample matrix have also been
102 described (Araujo, de Carvalho, Mota, de Araújo & Coelho, 2005, Bartroli, Escalada,
103 Jimenez-Jorquera & Alonso, 1991). These methods are based on the acid/base and
104 volatile nature of SO₂ and acetic acid, and their diffusion through a hydrophobic
105 permeable membrane. Being the analyte separated from the sample, indirect methods of
106 detection can be used as for example pH detection. The use of Ion Selective Field Effect
107 Transistors (ISFETs) for on-line measurements has been described and their advantages
108 (i.e. small size, fast response, long-term stability and easily integration in flow systems)
109 highlighted (Alegret, Bartrolí, Jiménez, del Valle, Domínguez, Cabruja & Merlos, 1991,
110 Gimenez-Gomez, P., et al., 2017).

111 Commercial analytical systems to determine these parameters in wines are based on
112 titration or absorbance colorimetric methods (AntonPaar, 2020, Foodlab, 2015, GAB,
113 2012). They provide fast-response and high accuracy, but they require laboratory
114 facilities, therefore they cannot be installed within the barrels in ageing wine cellars.

115 The aim of this work is to develop and validate a compact, automatic and rapid
116 microanalytical flow system for the determination of free sulfur dioxide and acetic acid
117 in winemaking industry. This system was planned to be placed in a wine barrel and
118 therefore it needed some special requirements of miniaturization and reduction of

119 reagents/sample consumption. For this reason, a flow cell assembly fabricated with low-
120 cost polymeric materials and integrating a gas-diffusion chamber and a pH-ISFET is
121 proposed. The system will enable winemakers' automatic sampling, conditioning and
122 analysis in the barrels, providing an accurate and fast determination method for free SO₂
123 and acetic acid. The flow system has been validated with wine samples by comparing
124 the results with those obtained by the official methods for both parameters, showing a
125 good agreement between them.

126 **2. Materials and Methods**

127 **2.1. Reagents and solutions**

128 All reagents are of high purity, analytical grade or equivalent and were
129 purchased from Sigma-Aldrich, unless stated otherwise. All solutions were prepared
130 using de-ionized water.

131 For the determination of acetic acid, stock solutions of 1 M acetic acid and 0.1
132 M potassium acetate (CH₃COOK) were prepared and renewed every 10 days. A
133 solution of potassium acetate containing 0.01 M KCl used as acceptor solution was
134 prepared every day from the stock solution of 0.1 M CH₃COOK. The calibration
135 solutions containing different concentrations of acetic acid in a range of 0.15 to 1.40 g
136 L⁻¹, were prepared every day from the 1 M stock solution, by diluting it in a background
137 solution containing the main species present in wines: 12 % (v/v) ethanol absolute, 0.12
138 mM KNO₃, 5.26 mM KH₂PO₄, 4.41 MgSO₄, 2.26 mM CaCl₂, 19.0 mM malic acid,
139 33.0 mM potassium bitartrate and 13.9 mM NaOH. This background solution was not
140 used for the free SO₂ method because was demonstrated that these species did not
141 interfere the pH-ISFET detection for the free SO₂ assays (Gimenez-Gomez, P., et al.,
142 2017). A 0.6 M HCl solution was used for adjusting the pH of the samples.

143 For the free sulfur dioxide determination, a solution containing 0.1 M sodium
144 hydroxide (NaOH), 5 % (v/v) glycerol and 0.1 M sodium sulfite (Na_2SO_3) was used as
145 stock for preparing the acceptor solution and was renewed every 10 days (Bartroli,
146 Escalada, Jorquera & Alonso, 1991). A solution containing 2×10^{-5} M Na_2SO_3 and 0.02
147 M sodium chloride (NaCl) was used as acceptor solution. The calibration solutions,
148 containing different concentrations of free SO_2 (5 – 60 mg L^{-1}), were prepared every
149 day from a stock solution of 400 mg L^{-1} of SO_2 diluted in a buffer solution containing
150 12 % (v/v) ethanol absolute (Panreac, Spain). The stock solution and the buffer solution
151 were provided by the company Biosystems (Spain). These solutions enabled the
152 stabilization of SO_2 during all the measurements. 2×10^{-6} M HCl and 0.6 M HCl
153 solutions were used for adjusting the pH of the acceptor solution to pH 6 and of the
154 sample below pH 1, respectively.

155 **2.2. Devices and flow system**

156 For pH detection a 3×3 mm^2 ISFET chip fabricated with standard
157 photolithographic techniques at the Instituto de Microelectrónica de Barcelona (IMB-
158 CNM, CSIC) (Jimenez, Abramova & Baldi, 2006, Jimenez-Jorquera, Orozco & Baldi,
159 2010,) was used. This chip was wired-bonded and encapsulated on a printed circuit
160 board (PCB) (Fig. S1, in the Supporting Information, SI) (Gutierrez, et al., 2010). A
161 double junction Ag/AgCl reference electrode (RE) (Orion 92-02-00, Thermo Fisher
162 Scientific Inc., Waltham, MA USA) was used. Potentiometric measurements were
163 performed with a portable homemade multi-ISFET meter readout fabricated at the IMB-
164 CNM (Gimenez-Gomez, Escudé-Pujol, Capdevila, Puig-Pujol, Jiménez-Jorquera &
165 Gutiérrez-Capitán, 2016). This readout (21 $\text{cm} \times 10$ $\text{cm} \times 3$ cm) enables the real-time
166 simultaneous measurement of six ISFETs by including the power supply unit, the digital
167 part and the analog part in the same device. The pH- ISFET measurement was carried

168 out by applying 100 μA and 0.5 V between the drain and the source, and recording the
169 ISFET gate potential (in mV). The visualization of the results was carried out by
170 employing a virtual instrument programmed with LabView 2013 (National Instruments,
171 Austin, USA).

172 A robust and portable flow system assembly containing the pH-ISFET, the RE
173 and the gas-diffusion chamber was designed and fabricated with two low-cost polymers:
174 poly (methyl methacrylate) (PMMA) and double-sided pressure-sensitive-adhesive
175 (PSA). The polymers were fast-mechanized by using a CO₂-laser writer (Epilog Mini
176 24, Epilog Laser, United States). The flow cell sized 3 cm width, 7 cm length and 2 cm
177 height, and was formed by two structures with different layers of PMMA and PSA (Fig.
178 1). The bottom structure was formed by 3 PMMA layers bonded together with 175- μm
179 thick PSA layers. The structure allowed the position of the microfluidic threads used as
180 sample inlet and outlet for the bottom side of the 150- μL gas-diffusion chamber (5 mm
181 width \times 10 mm length \times 3 mm height). A space for hosting the pH-ISFET was also
182 defined in this structure. Regarding the top structure, it was formed by 5 PMMA layers
183 also bonded with PSA layers of 175 μm . This contained another 150- μL gas-diffusion
184 chamber with the same dimensions as before, and a 7- μL cell for the pH-ISFET. The
185 flow channels (1 mm of diameter) were defined and connected to the top gas-diffusion
186 chamber, the pH-ISFET cell and the RE cell. In the top of the structure were defined the
187 microfluidic threads used as acceptor inlet for the top side of the gas-diffusion chamber,
188 and also the thread used as waste outlet of the system. Both fluidic PMMA/PSA
189 structures were fixed with 8 screws (1 mm diameter) to allow easy assembly and
190 disassembly of the system. O-ring junctions were used for the pH-ISFET, the RE and
191 the fluidic inlets and outlets in order to avoid the fluidic leakage. A hydrophobic
192 polyvinylidene fluoride (PVDF, VHP09050 Durapore®, 0.22 μm pore size, from Merck

193 Millipore, Germany) gas-permeable membrane (5 mm width×10 mm length) was placed
194 between the two symmetrical gas-diffusion chambers for separating the analyte from the
195 sample. The suitability of this membrane for gas-diffusion processes has been studied
196 previously (Gimenez-Gomez, P., et al., 2017). Two peristaltic pumps (403U/VM3,
197 Watson Marlow, UK) and Teflon pump tubes with an internal diameter of 1.0 mm
198 (Teknokroma, Barcelona, Spain) were used for driving the solutions.

199 A scheme of the fluidic design of the proposed device is depicted in Fig. 1c. This
200 flow system was the same for both parameters, but for SO₂ detection, an extra channel
201 with HCl for conditioning the acceptor solution was added.

202 **2.3. Detection methodology**

203 The detection methodology for both species is based on the use of the gas-
204 diffusion membrane to separate the analyte from the sample. This methodology exploits
205 the acid/basic characteristics of the analytes and their volatile gaseous state in their
206 acidic forms. In both cases, the diffusion ratio depends on the gas concentration, the
207 gradient and the contact time between both sides of the membrane, as well as on the pH
208 of the solutions. The main advantage of this method is the removing of matrix
209 interferences, resulting in a rapid detection method with low-reagent consumption.

210 **2.3.1. Acetic acid determination.**

211 The acetic acid/acetate equilibrium as function of pH is shown in Fig. S2a (in the
212 SI). The detection of the acetic acid is based on the conversion of all the acetate present
213 in the sample to its gas form (acetic acid) with the acidification of the sample to pH
214 below 1. Then, the acetic acid diffuses through the membrane and it is recollected by
215 the acceptor solution at around pH 6, converting all the acetic acid to CH₃COO⁻ plus
216 protons. If more acetic acid diffuses, the acceptor solution becomes more acidic. This

217 pH change is detected by the pH-ISFET and correlated with the concentration of acetic
218 acid in the sample.

219 As is shown in Fig. 1c, for acetic acid measurement, the sample or calibration
220 solution is injected in the bottom side of the cell and mixed 1:1 in volume with a 0.6 M
221 HCl solution to adjust the pH below 1 and convert all to acetic acid. The flow rate is 0.5
222 mL min⁻¹ (0.25 mL min⁻¹ each channel). The calibration solutions are performed in the
223 range from 0.15 to 1.40 g L⁻¹ of acetic acid. At the top side of the gas-diffusion
224 membrane, the acceptor solution was flowed at 0.5 mL min⁻¹.

225 The hydrodynamic conditions of the system and their effect on the diffusion rate
226 of the acetic acid were evaluated. Firstly, the study was carried out under continuous
227 flow conditions. For that, the acceptor (1×10⁻⁴ potassium acetate and 0.01 M KCl) and
228 the acidified sample (or calibration solution) with 0.6 M HCl were pumped during 7
229 min. Secondly, stop flow conditions were evaluated by using a colorimetric method
230 with a bromothymol blue acid/base colorimetric indicator and an image recorder. A 10⁻⁴
231 M potassium acetate acceptor solution with an excess of the colorimetric indicator and a
232 sample solution with a 1 g L⁻¹ of acetic acid was used. Both solutions were pumped and
233 kept in contact in both sides of the membrane during 10 min. The acceptor solution
234 chamber was recorded on video to evaluate diffusion process of the acetic acid under
235 stop flow conditions.

236 The chemical parameters of the acceptor solution were also optimized. For that,
237 three potassium acetate acceptor solutions (10⁻² M, 10⁻³ M and 10⁻⁴ M) containing 0.01
238 M KCl were checked with the hydrodynamics conditions previously optimized. The pH
239 of the acceptor solution in a range from 3 to 7 was also evaluated.

240 **2.3.2. Free SO₂ determination.**

241 The different forms of the sulfur dioxide (free and bounded) depend on the pH
242 (Fig. S2b, in the SI). As for the acetic acid detection, the determination of free SO₂ is
243 based on the conversion of all the bisulfite in the sample to its SO₂ gas form by
244 acidifying the sample to pH below 1. Then, SO₂ diffuses through the gas-diffusion
245 membrane and it is recollected by an acceptor solution adjusted to a pH value where
246 HSO₃⁻ is the predominant specie (pH 6), converting all the SO₂ to HSO₃⁻ plus protons.
247 The same as in the case of acetic acid, if more SO₂ diffuses, the acceptor solution
248 becomes more acidic. This pH change is detected by the pH-ISFET and the signal
249 variation (mV) is correlated with the concentration of free SO₂ in the sample.

250 As is shown in Fig. 1c, for free SO₂ measurement, the sample (or calibration
251 solution) is pumped and mixed 1:1 in volume with a 0.6 M HCl solution with a total
252 flow of 0.5 mL min⁻¹ (0.25 mL min⁻¹ each channel) for adjusting the pH below 1. The
253 acceptor solution is mixed 1:1 with 2×10⁻⁶ M HCl to get pH 6 with a total flow of 0.5
254 mL min⁻¹ (0.25 mL min⁻¹ each channel). Most of the chemical parameters and the
255 hydrodynamic conditions for the free SO₂ determination are used from a previous work
256 of our group (Gimenez-Gomez et al., 2017). These conditions were re-evaluated by
257 comparing the results obtained under continuous flow conditions during 10 min with
258 those obtained by flowing the solutions during 5 min and then stopping the flow during
259 2 min to enhance the diffusion in the chamber. Once selected the diffusion process, the
260 optimal measurement time under these conditions was also studied. For this
261 optimization, calibration solutions containing 5, 30 and 60 mg L⁻¹ of free SO₂ were
262 used.

263 **2.3.3. Acetic acid and free SO₂ determination in wine samples.**

264 Several sets of wines samples were used in order to test the feasibility of the
265 developed microanalytical flow system. Firstly, two commercial wines (a table red

266 wine, *Don Simón*, and a white wine with Apellation of Origin Penedés, Spain,
267 *Sumarroca*) were analyzed by spiking them with different concentrations of acetic acid
268 (0.00, 0.15, 0.50 and 1.00 g L⁻¹) and free SO₂ (0, 5, 10, 15 and 60 mg L⁻¹). The
269 percentage of recovery was calculated for each case

270 After that, the proposed system was validated by comparing the obtained results
271 of a set of samples with the official methods of the OIV for the free SO₂ and the acetic
272 acid. These analysis were carried out by the Institut Català de la Vinya i el Vi (IRTA–
273 INCAVI), which is an accredited laboratory (ISO 17025) in Catalonia. For the free SO₂
274 detection, the wines were analyzed by the Paul method (OIV, 2009a), by purging the
275 free SO₂ from the wine sample at low temperature (10 °C) with a stream of air (or
276 nitrogen). Then, the SO₂ was fixed and oxidized by bubbling through a dilute and
277 neutral H₂O₂ solution. Finally, the formed SO₂ was determined by titration with a
278 standard NaOH solution. For the acetic acid detection, the enzymatic method based on
279 the reaction of acid in presence of the coenzyme A (CoA) and adenosine triphosphate
280 (ATP), catalyzed by the acetyl–CoA synthetase (ACS) was used. The formed acetyl–
281 CoA (acetyl coenzyme A) reacted with oxaloacetate (catalyzed by the L-malic acid) to
282 produce reduced nicotinamide adenine dinucleotide (NADH). Finally, the NADH
283 concentration was determined by absorbance at 340 nm, and stoichiometrically related
284 to the acetic acid concentration in the sample (Megazyme, 2017, OIV, 2015). The
285 IRTA–INCAVI validates regularly both methods with a weekly analysis of real samples
286 duplicates. The accuracy of the method is determined by duplicate monthly analysis of a
287 standard solution and by the periodically measurement of uncertainty at 95 % calculated
288 from the results of intercomparison analysis with other accredited laboratories. The
289 standard solution used is prepared in the laboratory by making additions in a wine
290 matrix without SO₂ or acetic acid, depending on the analyte to determine. All the

291 accredited range is considered by changing the concentration every month. Therefore,
292 the interval of the standard methods includes the conditions of maximum variability
293 (different equipment, different people, different day), and the formula is directly
294 dependent on the concentration of SO₂ or acetic acid. Compared to the analysis that can
295 be performed in laboratories without accreditation, this method supposes a significant
296 advantage because it provides greater reliability of the results.

297 The first validation set was analyzed at the IRTA–INCAVI facilities with the
298 standard method and then transported to our institute. Five white wines (W1 to W5),
299 two red wines (R1 and R2) and two rosé wines (RO1 and RO2) were analyzed for this
300 first validation set. The samples W1, R1 and RO1 were also spiked with 0.7 g L⁻¹ of
301 acetic acid to evaluate the potential interference of acetic acid concentrations for the
302 free sulfur dioxide detection. The second validation set was analyzed at the IRTA-
303 INCAVI laboratories simultaneously with the proposed flow system in order to avoid
304 the evolution of the wine and the change in concentrations during the shipment and
305 storage. Four white wines (W6 to W9), five red wines (R3 to R7) and three rosé wines
306 (RO3 to RO5) were used in this validation. Although rosé wines are not aged in barrels,
307 they were used to validate the proposed flow system in all types of wines.

308 The procedure used for the analysis of the wine samples was as follows: firstly,
309 the microanalytical flow system was calibrated with three SO₂ calibration solutions (5
310 mg L⁻¹, 30 mg L⁻¹ and 60 mg L⁻¹) and acetic acid solutions (0.15 g L⁻¹, 0.70 g L⁻¹ and
311 1.40 g L⁻¹). Then, wine samples were consecutively analyzed and the recorded signals
312 were interpolated in the calibration plots to obtain the experimental results, which were
313 compared to those obtained by the standard method by the IRTA-INCAVI staff.

314 **3. Results and Discussion**

315 **3.1. Optimization of the system for acetic acid determination.**

316 First tests for acetic acid determination were carried out under continuous flow
317 conditions. The signal of each sample was recorded by the pH-ISFET, and the mean
318 signal value of the last 20 s was used to represent the calibration plot (data not shown).
319 The results showed a nonlinear fitting and an unstable signal indicating that under these
320 conditions there was not an efficient diffusion of the acetic acid from the sample to the
321 acceptor solution.

322 Therefore, stop flow conditions were checked to improve the response. For that,
323 an experiment using colorimetric detection to visualize the diffusion of acetic acid
324 through the membrane was performed. As can be seen in the Fig. S3 (in the SI), the
325 initial color of the solution containing the bromothymol blue (at $t = 0$ min) was blue (pH
326 above 8), indicating that the diffusion of the acetic acid has not initiated. After 5 min of
327 contact, the color of the acceptor solution became green, indicating that a fraction of the
328 acetic acid from the sample was diffused through the membrane and mixed with the
329 acceptor solution producing a decreasing pH (around 6.5–7). Finally, after 10 min, the
330 acceptor solution became totally yellow (pH < 6), meaning that all the acetic acid from
331 the sample passed through the membrane and was collected by the acceptor solution.
332 Therefore, the optimized time for stop flow conditions was fixed at 10 min for each
333 sample for next experiments.

334 Three different concentrations of potassium acetate (10^{-2} M, 10^{-3} M and 10^{-4} M)
335 in the acceptor solution were evaluated. This solution and the acidified sample were
336 flowed during 5 min. Then, the flow was stopped to let the acetic acid to diffuse through
337 the gas-diffusion membrane during 10 min. Afterwards, the acceptor solution was
338 flowed to the pH-ISFET cell by pumping during 10 s at 0.5 mL min^{-1} , and the signal

339 was recorded during 2 min in stop flow conditions. The mean value of the last 15 s was
340 used for the calibration plots in a range from 0.15 to 1.40 g L⁻¹ (Fig. S4, in the SI). A
341 linear response was obtained for the 10⁻³ M and 10⁻⁴ M potassium acetate, but for 10⁻²
342 M the linear fitting was poor (r = 0.870). The sensitivity obtained for 10⁻³ M potassium
343 acetate (-34.32 ± 1.15 mV dec⁻¹) was twice higher than that obtained for 10⁻⁴ M (-18.45
344 ± 2.10 mV dec⁻¹). The stability of consecutive measurements was also better for 10⁻³ M
345 (RSD 5.8%) than for 10⁻⁴ M (RSD 10.6%). Therefore, the optimal concentration of
346 potassium acetate in the acceptor solution was fixed to 10⁻³ M.

347 The pH of the acceptor solution for the acetic acid determination was also
348 evaluated and optimized. As shown in Fig. S2a (in the SI), acetic acid and acetate
349 coexist in the pH range from 3 to 7. A freshly prepared solution containing 10⁻³ M
350 potassium acetate and 0.01 M KCl had a pH value around 6, where acetate is the
351 predominant specie. Two adjusted pH solutions were tested, pH 5.5 and 7.0. From
352 results shown in Fig. S5 (in the SI), the non-adjusted acceptor solution presented a
353 sensitivity of -34.6 ± 1.1 mV dec⁻¹ (RSD 4.8%). Results obtained when the pH was
354 adjusted showed a decrease in the sensitivity (-23.9 ± 4.1 mV dec⁻¹ and -28.4 ± 3.0 mV
355 dec⁻¹, for pH 5.5 and 7, respectively). Besides, adjusted solutions showed a high
356 unstable signal with time, showing a RSD above 12% and 18% for the pH 7 and 5.5,
357 respectively. Therefore, a solution containing 10⁻³ M potassium acetate and 0.01 M KCl
358 without pH adjustment was used as acceptor solution for next assays.

359 The fluidic system was evaluated for acetic acid determination using the
360 optimized conditions described above (see Fig S.6, in the SI, for more details). The
361 acceptor solution (10⁻³ M CH₃COOK and 0.01 M KCl) and the sample solution (pH
362 below 1, acidified with 0.6 M HCl) were pumped during 5 min at 0.5 mL min⁻¹ (Fig
363 S.6i, in the SI). The flow was stopped during 10 min (Fig S.6ii, in the SI), and then, the

364 acceptor solution was flowed during 10 s at 0.5 mL min^{-1} to reach the pH-ISFET
365 chamber. Finally, the signal was recorded during two minutes (Fig S.6iii, in the SI) for
366 each concentration of acetic acid in the range from 0.15 to 1.4 g L^{-1} (Fig. 2a). Each
367 sample was measured by triplicated. A differential method was used for plotting the
368 calibration curves, which avoided the periodic use of control solutions. The analytical
369 signal was the difference between the mean value of the last 15 s of the sample solution
370 and the baseline (Fig. 2b). A linear variation of the potential in mV with the increasing
371 concentration of acetic acid was observed, with a sensitivity of $-32.4 \pm 1.8 \text{ mV dec}^{-1}$ ($r =$
372 0.999). The limit of detection (LOD) and the limit of quantification (LOQ), calculated
373 according to the IUPAC criterion for potentiometric sensors (Inczèdy, Lengyel & Ure,
374 1998), were 0.04 g L^{-1} and 0.12 g L^{-1} , respectively.

375 **3.2. Optimization of the system for free SO₂ determination.**

376 Most of the parameters were already optimized in a previous study (Gimenez-
377 Gomez, P., et al., 2017). A solution containing $2 \times 10^{-5} \text{ M Na}_2\text{SO}_3$ and 0.02 M sodium
378 chloride (NaCl) was used as acceptor solution, which pH was adjusted with $2 \times 10^{-6} \text{ M}$
379 HCl. To convert all the sulfites species of the sample into SO₂ gas, a 0.6 M HCl solution
380 was used for adjusting its pH below 1. Results obtained from the comparative study of
381 continuous and stop flow conditions are shown in Fig. S7 (in the SI). The determination
382 of free SO₂ was more efficient under continuous flow conditions ($-56.0 \pm 0.4 \text{ mV dec}^{-1}$;
383 $r = 0.999$) than under stop flow conditions ($-50.3 \pm 0.6 \text{ mV dec}^{-1}$; $r = 0.993$) due to the
384 higher drift of the baseline under later conditions. Moreover, the determination was
385 much faster under continuous flow conditions, therefore this methodology was chosen
386 for next experiments. The flow rate for each channel was selected at 0.25 mL min^{-1} . The
387 measurement time for one sample was optimized taking into account the stabilization of
388 the signal thus indicating that the diffusion of the SO₂ has been completed. For that,

389 triplicate calibrations were recorded in the range from 5 to 60 mg L⁻¹ of free SO₂ (Fig.
390 3a).

391 The signal recorded by the pH-ISFET was quite stable after 8 min for the
392 background solution (0 mg L⁻¹) and after 6 min for the calibration solutions (5, 30 or 60
393 mg L⁻¹). The use of the background solution after each assay guaranteed the perfect
394 cleaning of the flow system as shown by the recovery of the base line and provided also
395 the correction of drift. Therefore, these time conditions were fixed for the next
396 experiments. The analytical signal used was the difference between the mean value of
397 the last 15 s for each sample (or calibration solution) and for the background solution
398 (Fig. 3b). A linear variation of the potential with the increasing concentration of SO₂
399 was observed, with a sensitivity of -56.1 ± 0.5 mV dec⁻¹ ($r = 0.997$). The LOD and the
400 LOQ, calculated as before (Inczèdy, Lengyel & Ure, 1998), were 1.5 mg L⁻¹ and 4.5 mg
401 L⁻¹, respectively. The variation of potential for the whole concentration range
402 corresponded to more than 1 pH unit decreasing which is in agreement with theoretical
403 values under these conditions.

404 **3.3. Analysis of wine samples.**

405 **3.3.1. Determination of acetic acid.**

406 The acetic acid system was evaluated with two commercial wines and nine
407 wines samples provided by the IRTA-INCAVI. The content of acetic acid in
408 commercial wines was unknown, therefore solutions containing a fixed volume of wine
409 spiked with different concentrations of acetic acid were measured. The results obtained
410 for the two commercial wines (the red wine *Don Simón*, and the white wine *Sumarroca*)
411 are shown in Table S1 (in the SI). Theoretical values corresponded to the sum of the
412 initial experimental value calculated for the sample without spiking acetic acid and each

413 spiked concentration for this sample. According to the results, *Don Simón* red wine had
414 an acetic acid concentration around 0.56 g L^{-1} . This value had a perceptible deviation
415 (RSD 18%) due to the drift of the baseline. However, wine samples with spiked acetic
416 acid provided better results, with a RSD below 5%. The recovery values are above 98%
417 for 0.50 and 1.00 g L^{-1} spiked samples and 94% for 0.15 g L^{-1} spiked samples.
418 Regarding the *Sumarroca* white wine, it had an acetic acid concentration of 0.41 g L^{-1} .
419 Unlike the red wine *Don Simón*, the white wine *Sumarroca* presented a low relative
420 deviation (RSD 7%), meaning a more stable baseline. For the spiked samples, the RSD
421 was below 6% in all the cases. The recovery values for samples with an acetic acid
422 spiked concentration of 0.15 and 0.50 g L^{-1} were above 90%, while the recovery for the
423 sample spiked with 1.00 g L^{-1} was poorer (84%).

424 Results obtained from the test carried out with the set of wine samples provided
425 by IRTA-INCAVI are shown in Table S2 (in the SI). The repeatability of the proposed
426 flow system is quite good, showing a RSD below 10% for all the samples. Values
427 obtained with the flow system were lower (around 14–20% for all the samples) than the
428 obtained with the enzymatic method. This underestimation could be attributed to the
429 nature of samples provided by the IRTA-INCAVI. They had not completed the
430 fermentation process; therefore the concentration of acetic acid could have changed due
431 to evaporation and spontaneous evolution of the sample from their first analysis carried
432 out at the IRTA-INCAVI facilities.

433 **3.3.2. Determination of free SO_2 .**

434 The free SO_2 determination system was evaluated with two commercial wines
435 and nine wine samples provided by the IRTA-INCAVI laboratory. At first, the system

436 was calibrated in a range from 5 mg L⁻¹ to 60 mg L⁻¹. Then, each wine sample was
437 evaluated by triplicate and the recorded signal was interpolated in the calibration plot.

438 The same methodology used for acetic acid was applied here for commercial
439 wines: wine samples were spiked with 5, 10, 15 and 40 g L⁻¹ of SO₂. The results are
440 shown in Table S3 a (in the SI) for the red wine *Don Simón* and the white wine
441 *Sumarroca*. Theoretical free SO₂ concentration corresponds to the sum of the initial
442 concentration of wine calculated experimentally and the 70 % of added SO₂, assuming
443 that the other 30 % is bounded to aldehydes, ketones, sugars or acids present in wines
444 (Ribereau-Gayon, Dubourdiou, Donèche & Lonvaud, 2006a). According to the results
445 for the red wine *Don Simón*, this had a SO₂ concentration of around 23 mg L⁻¹ (RSD
446 8%). The recovery values obtained for the spiked samples were quite satisfactory
447 (above 90% in all cases) and stable (RSD below 7% in all the cases). From the results
448 for the *Sumarroca* white wine, the calculated initial concentration of the sample was 21
449 mg L⁻¹, with a RSD of 9%. The percentage of recovered acetic acid was above 95% for
450 all the cases, except for the 40 mg L⁻¹ addition (92 % of recovered SO₂). The RSD was
451 below 8% for all the spiked samples.

452 Another test to validate the microanalytical flow system for the free SO₂
453 detection was carried out with a set of red, white and rosé wine samples provided by
454 IRTA-INCAVI laboratory. Results were compared with those obtained with the
455 accredited Paul method (Table S4 in the SI). The repeatability of the flow system
456 method was good, with a RSD below 9% for all samples. Regarding the comparison of
457 values obtained for both methods, the error in percentage was in the range from 5% to
458 35%, with a predominant overestimation of free sulfur dioxide for the flow system.
459 Nevertheless, it is important to notice that all values of the flow system method were
460 within the confidence interval of the standard method. The highest differences (from

461 22% to 35%) were obtained for the three white wines samples (W1, W2 and W3) with a
462 concentration of free SO₂ below 12 mg L⁻¹ according to standard methods and from 12
463 to 15 mg L⁻¹ according to the flow method. This overestimation could be attributed to
464 the low concentration of free SO₂ of the sample, whose differences resulted in higher
465 relative errors.

466 On the other hand, the samples containing highest concentrations of acetic acid
467 (W1, R1 and R2, see Table S2) did not showed high relative errors between methods.
468 That means that the analysis of free SO₂ was not affected by the presence of high acetic
469 acid concentrations. The acceptor solution containing HSO₃⁻ is only affected by the
470 presence of SO₂ coming from the sample after its acidification. For white wines with a
471 concentration of free SO₂ above 20 mg L⁻¹, the difference between methods was lower
472 (below 13%). The difference between methods was from 0% to 5% and from 14% to
473 18% for red and rosé wines, respectively. There was a dispersion in the accuracy
474 (negative and positive) in rosé and red samples, which means that the difference
475 between both methods was not due to a systematic error. Besides, in samples spiked
476 with 0.7 g L⁻¹ of acetic acid after the SO₂ analysis (samples R1, W5 and RO2), the value
477 of free SO₂ changed below 5% for all samples, meaning that the acetic acid did not
478 interfere in the SO₂ detection in the proposed system. Despite these results, as in the
479 case of the acetic acid determination, these samples were measured by the IRTA-
480 INCAVI staff in their facilities, and then the samples were transported to the IMB-CNM
481 laboratory for the determination with the microanalytical flow system. During this time,
482 samples could have evolved, causing a change in the concentration of SO₂ from the
483 initial measurements, therefore some differences between methods could be attributed
484 to this fact.

485 3.3.3. Simultaneous determination of acetic acid and free SO₂.

486 After the individual analysis of the acetic acid and the free SO₂, a new set of
487 wine samples were analyzed to validate the system for the simultaneous detection of
488 both analytes against the official methods. All these analyses were carried out at the
489 IRTA-INCAVI laboratories in order to compare the results between methods in real
490 time then avoiding differences between methods caused by the evolution of the sample
491 with time. Once the system was calibrated for both species, 12 wine samples were
492 tested for acetic acid and free SO₂ consecutively.

493 Results of the comparative analysis are shown in Table 1 and Table 2 for acetic
494 acid and free SO₂, respectively. Acetic acid values presented a high dispersion of
495 results. For white wines the errors were high for the two sparkling wine samples (W6
496 and W9). This overvalue was due to the presence of carbonic acid that interferes in the
497 analysis due to the diffusion of this gas through the gas-diffusion membrane producing
498 a higher pH decreasing. A severe de-aeration method to remove the excess of carbonic
499 acid is not feasible in this case since free SO₂ and acetic acid could also be lost.
500 Therefore, the current method is not suitable for sparkling wines. Nevertheless,
501 considering that a low number of white wines follow the process of ageing and these are
502 never sparkling wines, we cannot consider this interference for the proposed application
503 in this work. However, for the two other white wine samples (W7 and W8), the
504 correlation between both methods was high. For red wine samples, values were in good
505 agreement with the obtained by the standard method with an error below 12% in all the
506 cases. The different signal of relative error indicated that there was not a systematic
507 error associated. For rosé wine samples, the accuracy between methods was high for
508 two of the three samples (RO3 and RO5), but the different signal meant also that there
509 was not a systematic error associated. It could be associated to some matrix effect due to
510 the composition of the rosé wines, affecting the diffusion of the acetic acid.

511 Regarding the values obtained for the free SO₂ for white wines samples, the
512 dispersion of errors is also high. For W8 sample, the error is high, maybe due to the low
513 concentration of free SO₂ in this sample. For sparkling white wines (W6 and W9), the
514 positive error indicated a slight effect of carbonic gas as interfering, as was discussed
515 above for the acetic acid detection. Concerning the results obtained for red wine
516 samples, the results obtained with the flow system were similar to those obtained with
517 the standard method, with low differences for samples R4, R5, R6 and R7. The sample
518 R3 showed a slightly higher difference, but the experimental value obtained with the
519 flow system was within the confidence interval of the IRTA-INCAVI measurements,
520 demonstrating the good agreement between methods for this case too. It is worthwhile
521 to notice that for red wine samples with low concentration of free SO₂ (R7, 4 mg L⁻¹),
522 the values for the flow system were similar to the standard ones, demonstrating the
523 suitability of the method for the entire range of red wines. For rosé wines, the difference
524 between both methods was also low for RO3 and RO4. However, if we consider the
525 confidence interval the value is quite similar for RO5 in both methods. Therefore, we
526 can conclude that in general and mostly for low concentrations, the values for the flow
527 system are in agreement or even higher than that for standard method. That suggests
528 that the diffusion of the SO₂ is not affected in this case by the composition of the
529 sample.

530 The data obtained with the microanalytical flow system, for each type of wine,
531 was plotted versus that obtained with the standard method (Fig. 4). The differences
532 between both methods were analyzed by the least squares method (Table S5, in the SI).
533 Regarding the acetic acid, samples W6, W9 and RO5 were not included in the analysis,
534 thus only the red wines were analyzed by the least square method. The slope obtained
535 was acceptable (0.71 ± 0.06), with an intercept close to zero (0.12 ± 0.03 g L⁻¹). The

536 positive value of the intercept was due to a certain overestimation of the values for the
537 flow system for low concentrations of acetic acid.

538 Regarding the free SO₂, data from W8 was removed for the analysis. There was
539 a good agreement between both methods for white wine samples. The slope was above
540 1 (1.4 ± 0.1), due to the slightly overestimation of the value calculated by the flow
541 system. Although it is important to notice again that all values of the flow system
542 method were within the confidence interval of the standard method. From the analysis
543 of white wine samples could be concluded that the developed method in its current form
544 was accurate enough to be applied in white samples not containing very low
545 concentration of free SO₂. For red wine samples, the slope was very close to the ideality
546 (1.0 ± 0.1), and the intercept was almost zero ($0.2 \pm 1.0 \text{ mg L}^{-1}$), demonstrating the great
547 competence of the developed system. For rosé wines, results are also good. The slope
548 and the intercept were close to one and zero, respectively (1.0 ± 0.12 and $-1.0 \pm 2.0 \text{ mg}$
549 L^{-1}). The uncertainty intervals were through the ideal value, indicating a no-systematic
550 deviation between methods.

551 **3.4. Hydrodynamic parameters for the aging in barrels.**

552 Regarding the hydrodynamic performance of the flow system, only one gas-
553 diffusion membrane was used during the complete validation of the system,
554 demonstrating the robustness of this membrane as was observed in our previous work
555 for the free and total SO₂ determination (Gimenez-Gomez, P., et al., 2017). Volumes of
556 solutions consumed for each assay of the process were as follows: To calibrate the
557 system, the volume of the reagents used is below 10.5 ml in all the cases. Then, 1.5 ml
558 of each wine sample and below 3.5 ml of all the involved reagents were consumed for
559 each assay. In the case of acetic acid, below 15 ml of all the reagents were consumed to
560 calibrate the system. Then, 1.25 ml of wine sample and reagents were consumed per

561 assay. The volumes used of each solution were chosen for injecting three times the
562 volume of the new solution in comparison to the volume within the microfluidic
563 channels. In this way, the perfect renovation of the fluidic microchannels with next
564 solutions was guaranteed, avoiding the memory effect for the sensor from previous
565 assays by removing any trace of SO₂ or acetic acid coming from them.

566 From these numbers, and considering one assay per day to control the
567 concentration of free SO₂ and acetic acid within the barrel, if 1 L containers are used for
568 each reagent/solution, the microanalytical flow system can work up to three months
569 without any user intervention. Taking into account that wine ageing in winemaking
570 industry normally takes up to 18 months depending of the wine, it will be necessary to
571 substitute some of the solution containers six times at most during the full process,
572 without manipulating the barrels and avoiding risks for the wine quality. The quality of
573 the wine is also maintained because the proposed method needs to take up low volumes
574 of samples from the barrel, avoiding the refill of the barrels of current systems.
575 Therefore, this new microanalytical flow system for the simultaneous determination of
576 acetic acid and free SO₂ can be a suitable and a feasible tool for controlling excessive
577 oxidation processes or detection of spoilage microorganism metabolism in red and
578 white wines during ageing in barrels, preventing aroma and flavor deviations.

579 **4. Conclusions**

580 A new microanalytical flow system for monitoring free SO₂ and acetic acid
581 concentration in wines samples has been developed and evaluated. This system
582 incorporates a permeable gas-diffusion membrane to separate the analyte from the
583 sample avoiding interferences and uses as detector a pH-ISFET. Profiting the acid/basic
584 characteristics of the analytes and the volatile nature of the acidic form, indirect
585 detection of pH is carried out. The system was optimized in a range from 5 mg L⁻¹ to 60

586 mg L⁻¹ and from 0.15 g L⁻¹ to 1.40 g L⁻¹, for free SO₂ and acetic acid, respectively, in
587 accordance with the expected values in the winemaking industry. This was validated
588 with several set of wine samples, and comparing the results with those obtained with
589 standard methods. Values for acetic acid showed quite good correlation for red wine
590 between both methods. For white wines, the correlation between methods was also
591 good, except for samples containing carbonic acid, which interfered the detection and
592 caused a high overestimation of the acetic acid value, as was also observed for the free
593 SO₂ detection. For rosé wines, in general, experimental results showed higher
594 differences in comparison with the standard method. This fact could be attributed to the
595 composition of rosé wines affecting the diffusion rate of the acetic acid. Regarding free
596 SO₂ determination, the correlation between methods was quite good for white wines,
597 except for those samples with low concentration of free SO₂ (according to the standard
598 method). In that case the flow system overestimated the concentration given by the
599 standard method. For red and rosé wines the correlation between methods was quite
600 good, demonstrating the good agreement between the compared methods.

601 Therefore, the results in this work demonstrated the high potential of the
602 developed microanalytical flow system for monitoring acetic acid and free SO₂ in the
603 field of the winemaking industry, mostly in red wines. The accuracy of the proposed
604 flow system is appropriate for the considered application: the periodic control of both
605 parameters in aging barrels for red and some white wines, allowing corrective actions to
606 be carried out in real time if it were necessary. The size of the system allows its easy
607 integration within ageing barrels, enabling the calibration and wine measurements in an
608 automated mode. Besides, the use of pH-ISFET provides added advantages for the
609 proposed application, like low cost, reproducibility and robustness, making the system
610 fabrication and maintenance costs effectively low. The low volume required for each

611 analysis enables a long-term autonomy of the device. Thereupon, this proposed
612 approach could be a promising alternative to traditional methods of wine control in the
613 winemaking industry, especially for the monitoring of red wines in barrels, which are
614 the most common variety of wines aged in barrels.

615 **Credit authorship contribution statement**

616 **Pablo Giménez-Gómez:** Management, Coordination, Investigation, Methodology,
617 Experimental, Data curation, Supervision, Writing - review & editing. **Manuel**
618 **Gutiérrez-Capitán:** Supervision, Draft writing. **Juan Manuel Ríos:** Methodology,
619 Coordination, Experimental. **Fina Capdevila:** Methodology, Experimental, Wine
620 samples, Draft writing. **Anna Puig-Pujol:** Methodology, Experimental, Wine samples,
621 Draft writing. **Cecilia Jiménez-Jorquera:** Supervision, Draft writing, Funding
622 acquisition.

623

624 **Declaration of Competing Interest**

625 The authors declare that they have no known competing financial interests or
626 personal relationships that could have appeared to influence the work reported in this
627 paper.

628

629 **Acknowledgements**

630 We acknowledge funding from the Spanish R & D Na-tional Program
631 (MINECO, Project RTI2018-100773-B-C31) and from Sapere Corporation (California,
632 USA). We also acknowledge the BioSystems Company for providing us stable home-
633 made solutions to carry out the long-terms measurements. This work used the Spanish

634 ICTS Network MICRONANOFABS and was partly supported by the Spanish Ministry
635 of Economy, Industry and Competitiveness.

636

637 **Appendix A. Supplementary data**

638 The following is **Supplementary data to this article:.....**

639

640 **References**

641 Adams, J.B. (1997). Food additive-additive interactions in-volving sulphur dioxide and
642 ascorbic and nitrous acids: A review. *Food Chemistry*, 59(3), 401-409.

643 [https://doi.org/10.1016/S0308-8146\(96\)00283-X](https://doi.org/10.1016/S0308-8146(96)00283-X)

644 Adeloju, S.B. & Hussain, S. (2016). Potentiometric sulfite biosensor based on
645 entrapment of sulfite oxidase in a polypyrrole film on a platinum electrode modified
646 with platinum nanoparticles. *Microchimica Acta*, 183(4), 1341-1350.

647 <https://doi.org/10.1007/s00604-016-1748-0>

648 Alegret, S., Bartrolí, B., Jiménez, C., del Valle, M., Domínguez, C., Cabruja, E. &
649 Merlos, A. (1991). Flow-through pH-ISFET as detector in automated determinations.

650 *Electroanalysis*, 3(4-5), 349-354. <https://doi.org/10.1002/elan.1140030417>

651 AntonPaar. (2020). *FTIR wine analyzer: Lyza 5000 Wine*. Retrieved from:
652 <https://www.anton-paar.com/corp-en/products/details/lyza-5000-wine/>.

653 Araujo, C.S.T., de Carvalho, J.L., Mota, D.R., de Araújo, C.L. & Coelho, N.M.M.
654 (2005). Determination of sulphite and acetic acid in foods by gas permeation flow
655 injection analysis. *Food Chemistry*, 92(4), 765-770.

656 <https://doi.org/10.1016/j.foodchem.2004.10.032>

657 Bakker, J., Bridle, P., Bellworthy, S.J., Garcia-Viguera, C., Reader, H.P. & Watkins,
658 S.J. (1998). Effect of sulphur dioxide and must extraction on colour, phenolic

659 composition and sensory quality of red table wine. *Journal of the Science of Food*
660 *and Agriculture*, 78(3), 297-307. [https://doi.org/10.1002/\(SICI\)1097-](https://doi.org/10.1002/(SICI)1097-)
661 0010(199811)78:3<297::AID-JSFA117>3.0.CO;2-G

662 Bartoli, J., Escalada, M., Jimenez-Jorquera, C. & Alonso, J. (1991). Determination of
663 total and free sulfur-dioxide in wine by flow-injection analysis and gas-diffusion
664 using para-aminoazobenzene as the colorimetric reagent. *Analytical Chemistry*,
665 63(21), 2532-2535. <https://doi.org/10.1021/ac00021a026>

666 Eschenbruch, R. (1974). Sulfite and sulfide formation during winemaking-Review.
667 *American Journal of Enology and Viticulture*, 25(3), 157-161.

668 Fazio, T. & Warner, C.R. (1990). A review of sulfites in foods - Analytical
669 methodology and reported findings. Food Additives and Contaminants Part a.
670 *Chemistry Analysis Control Exposure & Risk Assessment*, 7(4), 433-454.
671 <https://doi.org/10.1080/02652039009373907>

672 FOODLAB®. (2015). *CDR WineLab® System*. Retrieved from:
673 <https://www.cdrfoodlab.com/foods-beverages-analysis/volatile-acidity-wine/>.

674 GAB System. (2012). *Tenamatic GAB Automatization module for Garcia-Tena method*
675 *for volatile acidity*. Retrieved from:
676 <http://shop.gabsystem.com/b2c/producto/1010016/2/tenamatic-gab>.

677 Gimenez-Gomez, P., Escudé-Pujol, R., Capdevila, F., Puig-Pujol, A. Jiménez-Jorquera,
678 C. & Gutiérrez-Capitán, M. (2016). Portable Electronic Tongue Based on
679 Microsensors for the Analysis of Cava Wines. *Sensors*, 16(11), 1796.
680 <https://doi.org/10.3390/s16111796>

681 Gimenez-Gomez, P., et al. (2017). Analysis of free and total sulfur dioxide in wine by
682 using a gas-diffusion analytical system with pH detection. *Food Chemistry*, 228,
683 518-525. <https://doi.org/10.1016/j.foodchem.2017.02.026>

684 Gutierrez, M., et al. (2010). Hybrid electronic tongue based on optical and
685 electrochemical microsensors for quality control of wine. *Analyst*, 135(7), 1718-
686 1725. <https://doi.org/10.1039/C0AN00004C>

687 Inczèdy, J., Lengyel, T. & Ure, A.A. (1998). *Compendium of analytical nomenclature*
688 *IUPAC*. Oxford Blackwell Science.

689 Jimenez, C., Abramova, N. & Baldi, A. (2006). ISFET based sensors: fundamentals and
690 applications. In Grimes, C.A., Dickey, E.C. & Pishko, M.V. (Eds.), *Encyclopedia of*
691 *Sensors*. American Scientific Publishers.

692 Jimenez-Jorquera, C., Orozco, J. & Baldi, A. (2010). ISFET Based Microsensors for
693 Environmental Monitoring. *Sensors* 10(1), 61-83.
694 <https://doi.org/10.3390/s100100061>

695 Li, H. et al. (2019). Disposable stainless steel-based electro-chemical microsensor for in
696 vivo determination of indole-3-acetic acid in soybean seedlings. *Biosensors &*
697 *Bioelectronics*, 126, 193-199. <https://doi.org/10.1016/j.bios.2018.10.041>

698 Megazyme. (2017). *Acetic Acid Assay Kit*. Retrieved from:
699 <https://www.megazyme.com/acetic-acid-assay-kit-acs-manual-format> Morata, A.
700 (2019). *Red Wine Technology (1st ed.)*. Elsevier..

701 OIV: International Organisation of Vine and Wine (2009a). Compendium of
702 International Methods of Analysis of Wines and Musts. Sulphur dioxide-titrimetry:
703 OIV-MA-AS323-04A.

704 OIV: International Organisation of Vine and Wine (2009b). Compendium of
705 International Methods of Analysis of Wines and Musts. Sulphur dioxide-iodometry:
706 OIV-MA-AS323-04B.

707 OIV: International Organisation of Vine and Wine (2009c). Compendium of
708 International Methods of Analysis of Wines and Musts. Sulphur dioxide-molecular
709 method: OIV-MA-AS323-04C

710 OIV: International Organisation of Vine and Wine (2010). Guidelines on automated
711 colorimetric analyzers in enology: OIV/OENO 391/2010.

712 OIV: International Organisation of Vine and Wine (2015). Compendium of
713 International Methods of Analysis of Wines and Musts. Volatile acidity: OIV-MA-
714 AS313-02.

715 OIV: International Organisation of Vine and Wine (2017). International code of
716 enological practices.

717 Ribereau-Gayon, P., Dubourdieu, D., Donèche B., Lonvaud, A. (2006a). *Handbook of*
718 *Enology (2nd ed.)*. John Wiley & Sons (Vol. 1, The Microbiology of Wine and
719 Vinifications).

720 Ribereau-Gayon, P., Glories, Y., Maujean, A. & Dubourdieu, D. (2006b). *Handbook of*
721 *Enology (2nd ed.)*. John Wiley & Sons (Vol. 2, Chemistry of Wine - Stabilization
722 and Treatments).

723 Sroysee, W., Ponlakheth, K., Chairam, S., Jarujamrus, P. & Amatatongcha, M. (2016) A
724 sensitive and selective on-line amperometric sulfite biosensor using sulfite oxidase
725 immobilized on a magnetite-gold-folate nanocomposite modified carbon-paste
726 electrode. *Talanta*, 156, 154-162. <https://doi.org/10.1016/j.talanta.2016.04.066>
727
728

729 **Table 1.** Values of acetic acid concentration obtained with the microanalytical flow
 730 system and with the standard accredited potentiometric method for 12 wine samples.
 731 The confidence intervals are calculated with a level of 95% for the standard method.

Wine ¹	Acetic acid concentration (g L ⁻¹)		
	Microanalytical flow system	Standard method ²	Relative error %
W6 ^a	0.52	0.18 ± 0.02	190
W7	0.31	0.29 ± 0.04	7
W8	0.17	0.17 ± 0.02	1
W9 ^a	1.54	0.23 ± 0.03	569
R3	0.44	0.47 ± 0.06	-7
R4	0.30	0.26 ± 0.03	12
R5	0.64	0.70 ± 0.09	-8
R6	0.32	0.26 ± 0.03	10
R7	0.73	0.70 ± 0.09	4
RO3	0.37	0.29 ± 0.04	26
RO4	0.25	0.24 ± 0.03	2
RO5	0.20	0.35 ± 0.04	-43

732 ¹W: white wine; R: red wine; RO: rosé wine

733 ²Confidence interval calculated by IRTA-INCAVI from the results of inter-comparison
 734 analysis

735 ^asparkling

736

737

738 **Table 2.** Values of free SO₂ concentration obtained with the microanalytical flow
 739 system and with the standard accredited Paul method for 12 wine samples. The
 740 confidence intervals are calculated with a level of 95% for the standard method.

Wine ¹	Free SO ₂ concentration (mg L ⁻¹)		
	Microanalytical flow system	Standard method ²	Relative error %
W6 ^a	25	22 ± 7	14
W7	18	19 ± 6	-5
W8	22	5 ± 2	340
W9 ^a	56	46 ± 14	22
R3	13	11 ± 4	18
R4	15	15 ± 5	0
R5	26	25 ± 8	4
R6	14	15 ± 5	-7
R7	4	4 ± 2	0
RO3	5	5 ± 2	0
RO4	17	19 ± 6	-11
RO5	3	6 ± 2	-50

741 ¹W: white wine; R: red wine; RO: rosé wine

742 ²Confidence interval calculated by IRTA-INCAVI from the results of inter-comparison
 743 analysis

744 ^asparkling

745

746

747 **Figure Captions**

748 **Fig. 1.** Design of the flow system. (a) Scheme of the flow chamber for free SO₂ and
749 acetic acid determination with the top and bottom structures; (b) Picture of the
750 assembled analytical device. (c) Scheme of the fluidic performance of the
751 microanalytical device. (*) The channel containing 2×10^{-6} HCl is only used for the free
752 SO₂ detection.

753 **Fig. 2.** Analytical response for acetic acid. (a) pH-ISFET recording and (b) the obtained
754 calibration curve for 0, 0.15, 0.20, 0.40, 0.70 and 1.40 g L⁻¹ acetic acid solutions. The
755 numbers inside the plot (a) represent the concentration of acetic acid (g L⁻¹). Standard
756 deviation of triplicated calibrations is drawn as error bars.

757 **Fig. 3.** Analytical response for free SO₂. (a) pH ISFET recording and b) the obtained
758 calibration curve for 0, 5, 30 and 60 mg L⁻¹ SO₂ solutions. The numbers inside the plot
759 (a) represent the concentration of free SO₂ (mg L⁻¹). Standard deviation of triplicated
760 calibrations is drawn as error bars.

761 **Fig. 4.** Plot representing the data of the standard method vs. the microanalytical flow
762 system for free SO₂ determination. The dotted line corresponds to the ideal correlation
763 between methods. Red, green and blue filled squares correspond to red, rosé and white
764 wine samples, respectively.

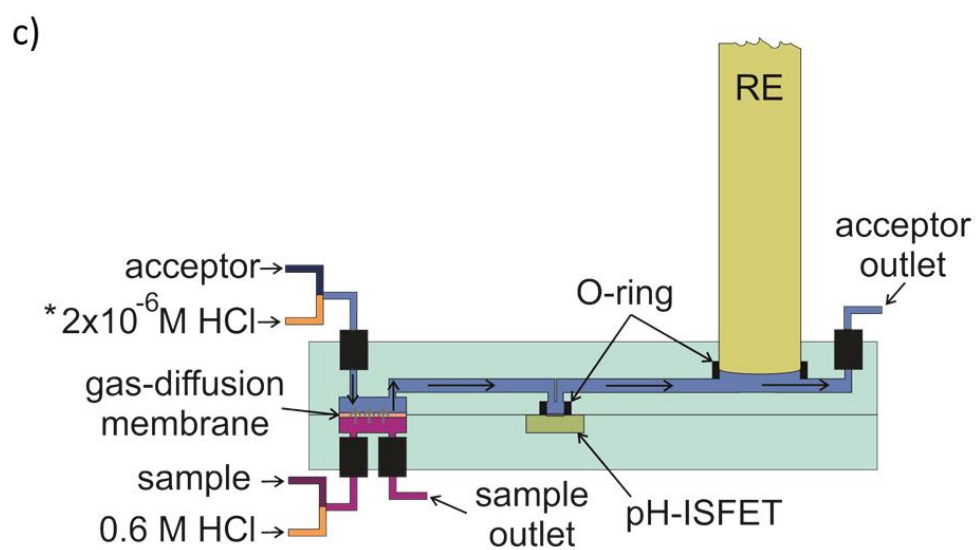
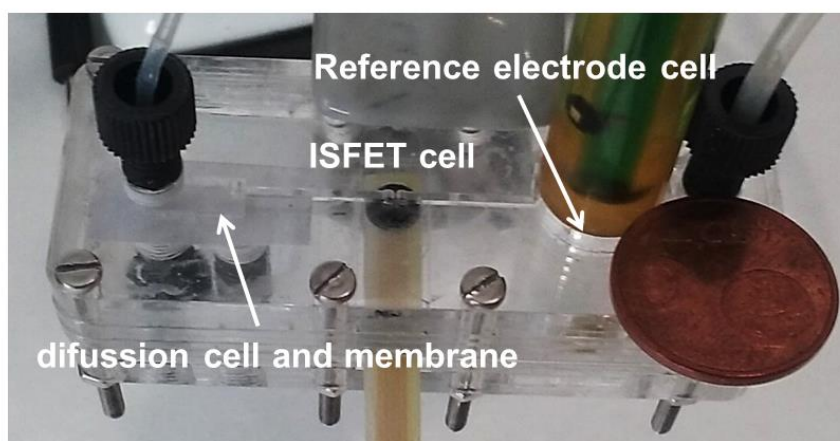
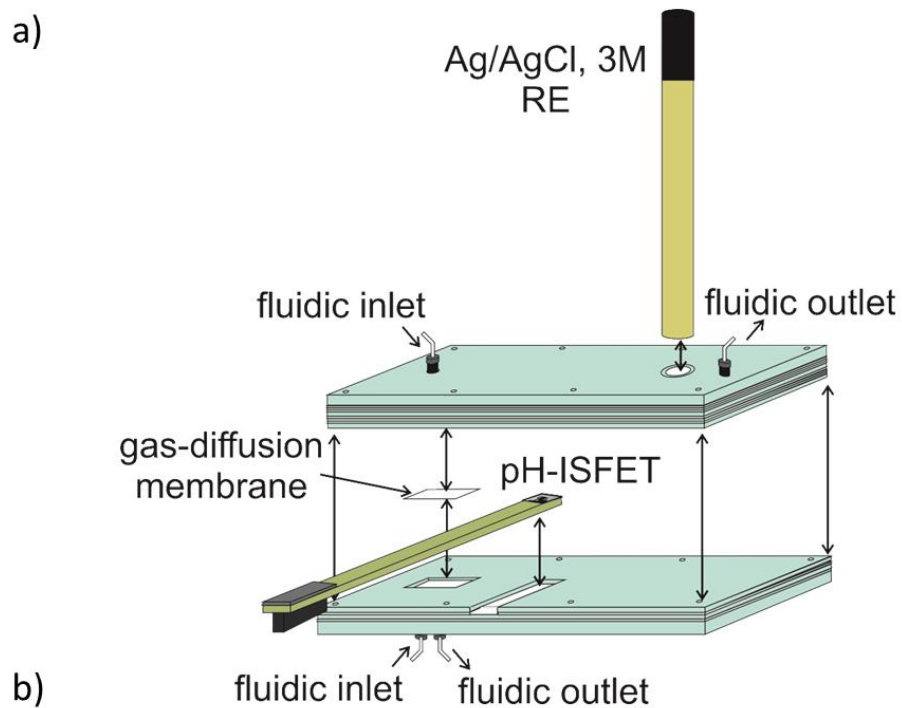
765

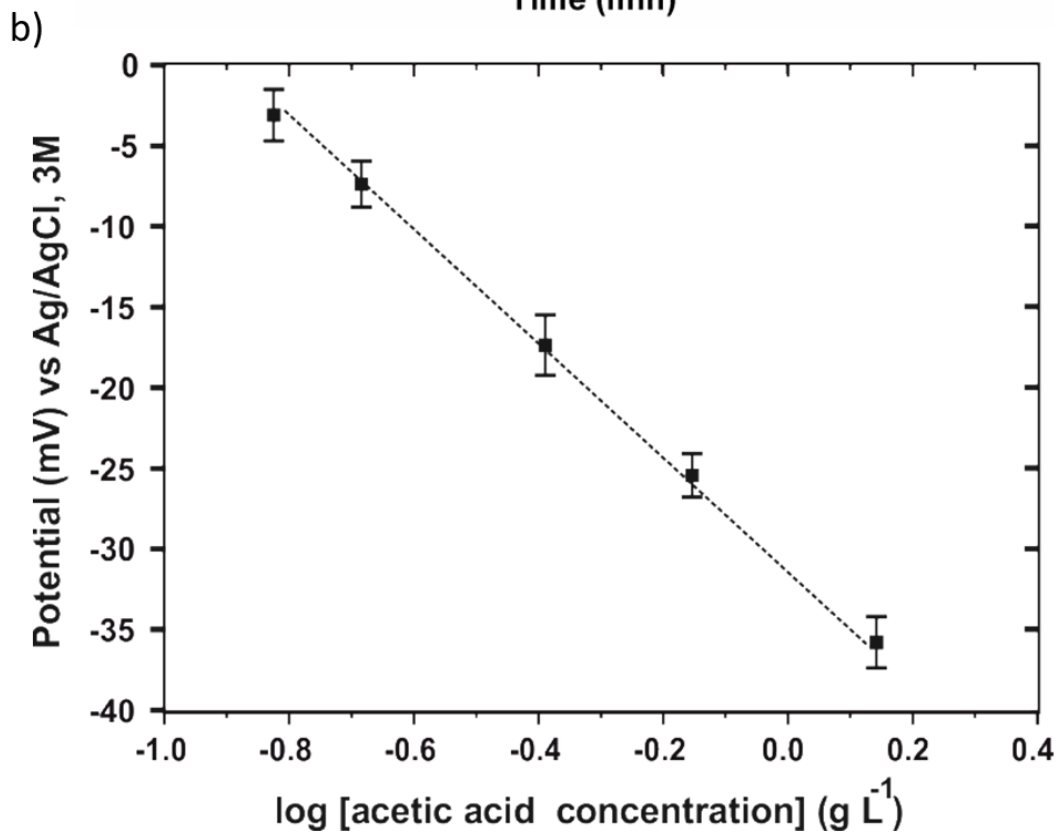
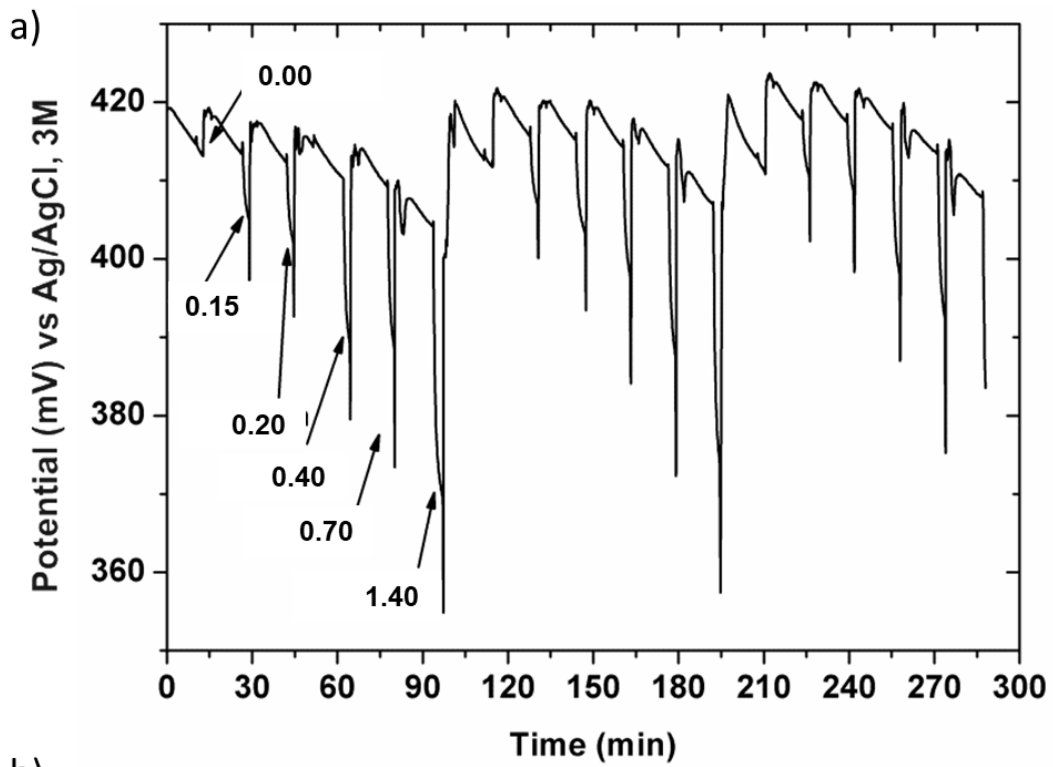
766

767

768

769

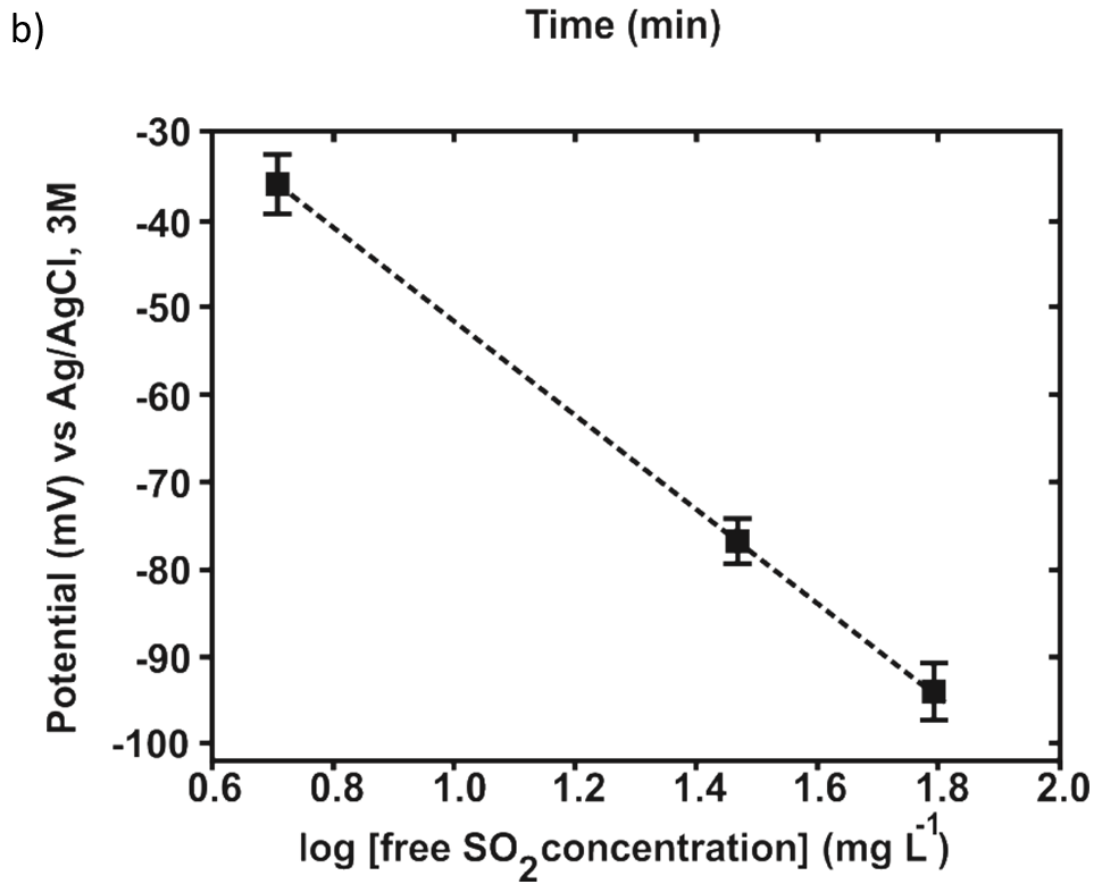
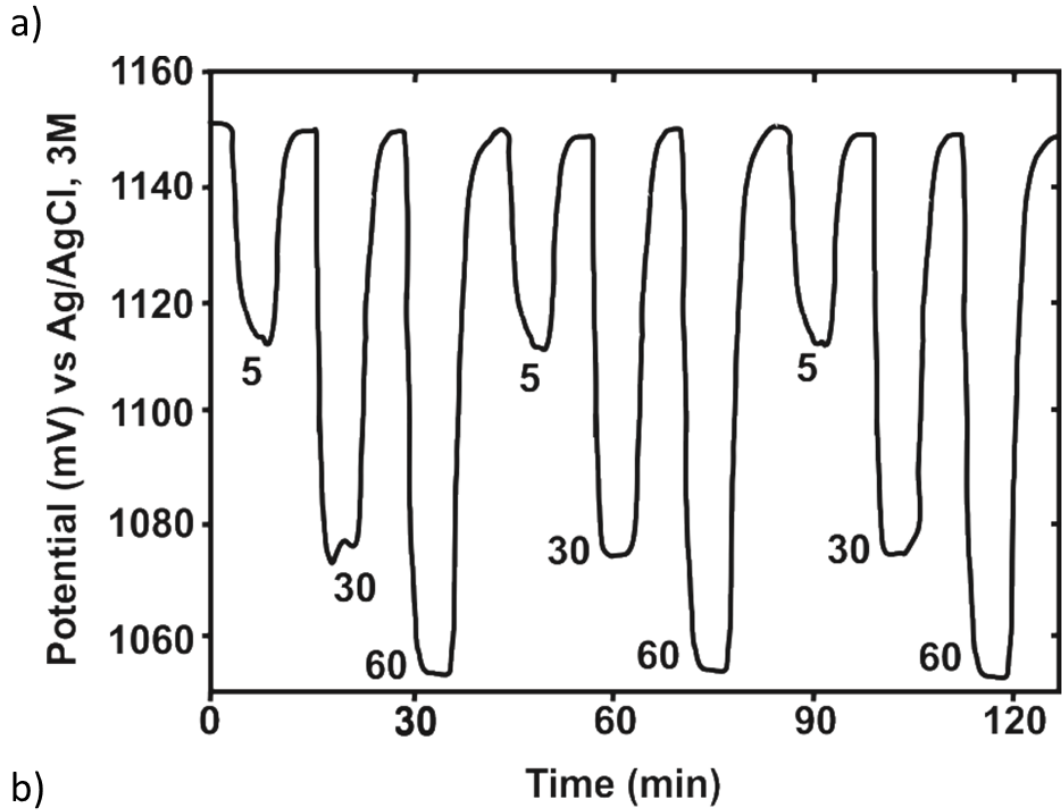




771

772

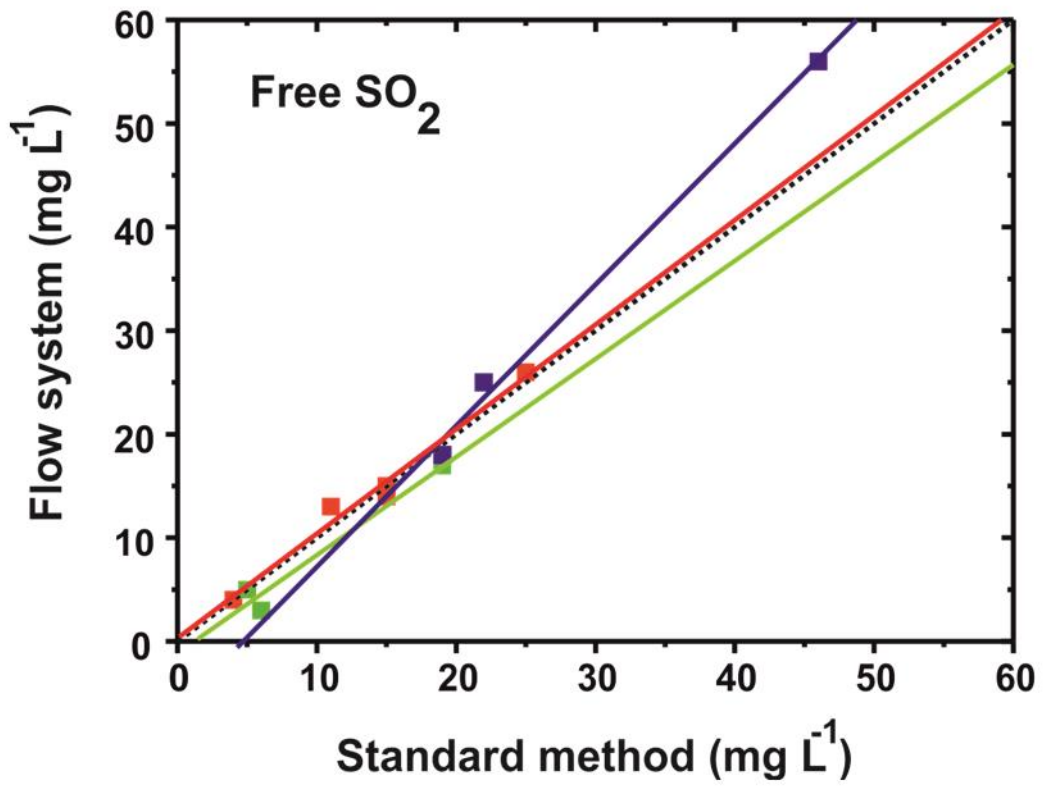
773



774

775

776



777

INDEX OF SUPPLEMENTARY INFORMATION

Fig. S1. Detail of the pH-ISFET used in this work.

Fig. S2. Different forms of sulfur dioxide and acetic acid as function of the pH.

Fig. S3. Colorimetric detection using bromothymol blue as pH indicator to visualize the diffusion of acetic acid through the gas-diffusion membrane.

Fig. S4. Results obtained for the potassium acetate concentration optimization in the acceptor solution used for acetic acid determination.

Fig. S5. Results obtained in the study of the pH effect of the acceptor solution in the acetic acid determination.

Fig. S6. Detail of one analytical response obtained during the acetic acid determination.

Fig. S7. Results for the comparative study of continuous and stop flow conditions for the free SO₂ detection.

Table S1. Results obtained for the commercial wine *Don Simón* and the commercial wine DO Penedés, Spain, *Sumarroca*, spiked with different concentrations of acetic acid.

Table S2. Results of acetic acid concentration obtained for wines samples provided by the IRTA-INCAVI, and compared with the standard method.

Table S3. Results obtained for the commercial wine *Don Simón*, and the wine DO Penedés, Spain, *Sumarroca*, spiked with different concentrations of sulfur dioxide.

Table S4. Results of free SO₂ concentration obtained for wines samples provided by the IRTA-INCAVI and compared with the standard method.

Table S5. Values of the least squares method comparing the microanalytical flow system and the standard method for acetic acid and free SO₂ determination.

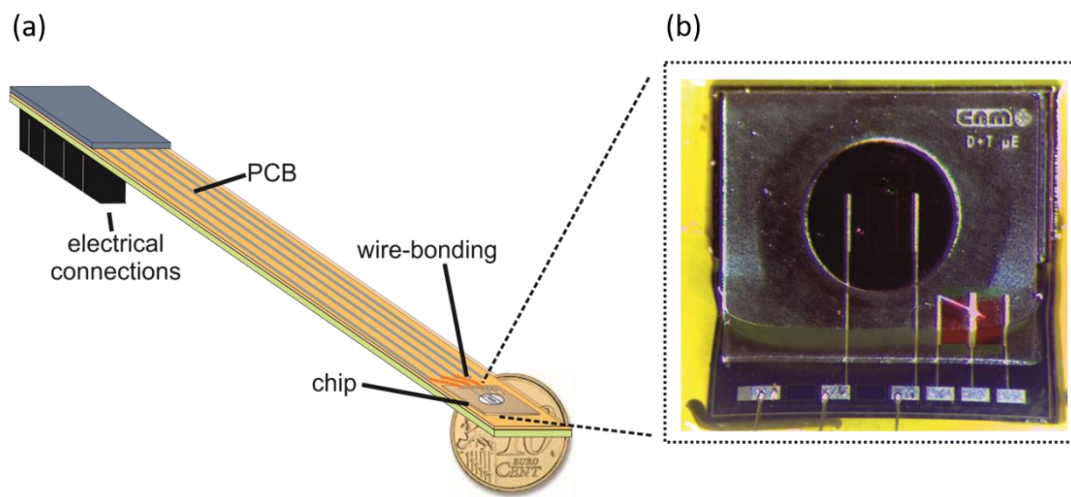
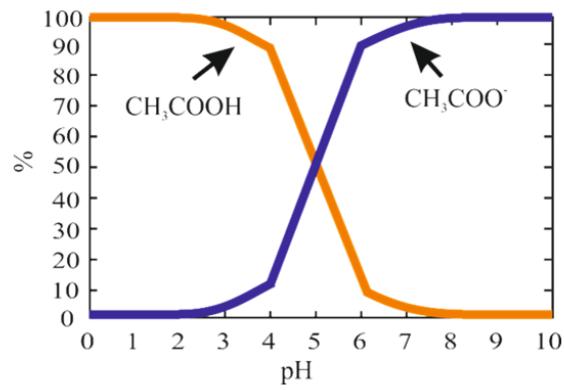


Fig. S1. (a) Drawing of the encapsulated pH-ISFET on a PCB and (b) picture detailing the pH-ISFET chip.

a)



b)

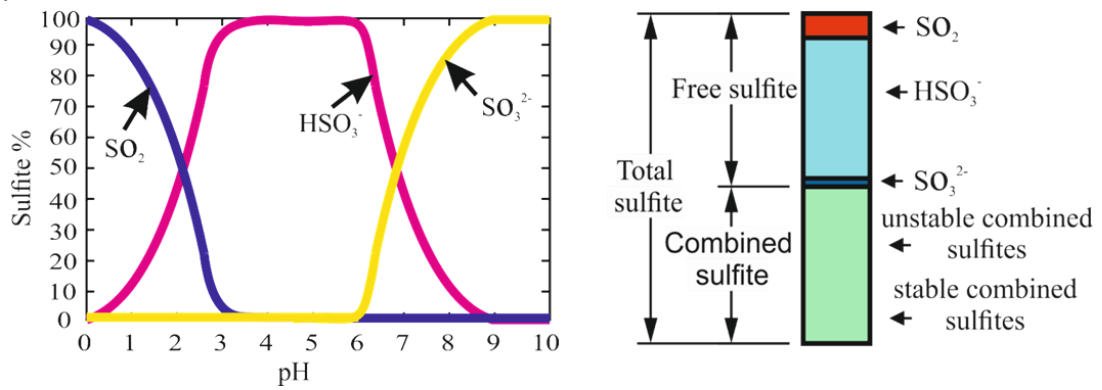


Fig. S2. (a) Percentage of the chemical forms of sulfite as function of pH and scheme of the different chemical forms of sulfite in real wine. (b) Percentage of acetic acid and acetate as function of pH.

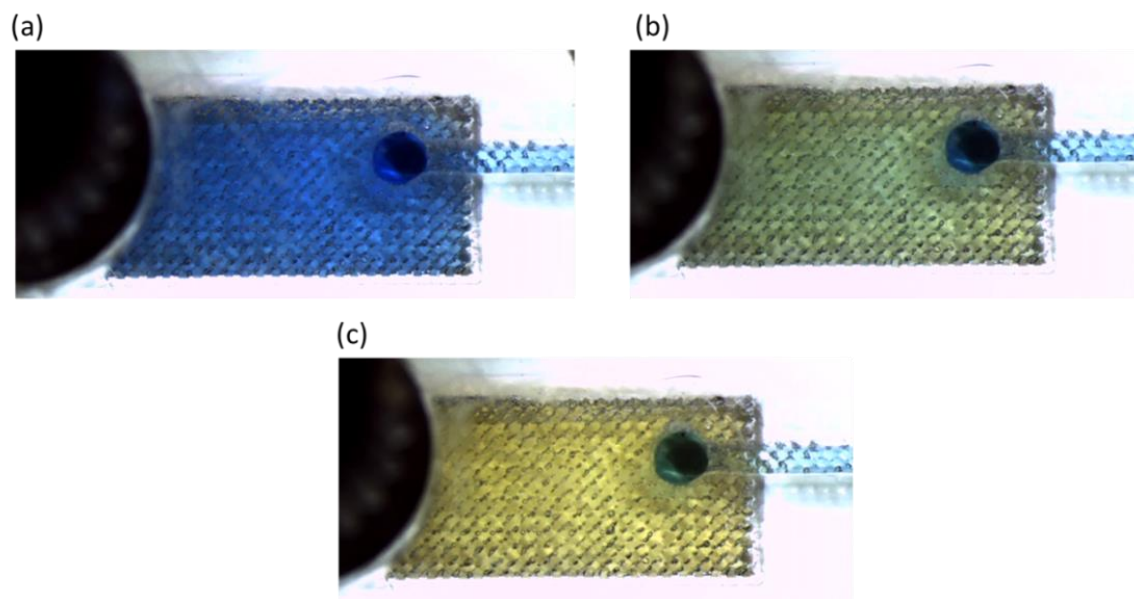


Fig. S3. Pictures of the acceptor solution chamber recorded on video in presence of bromothymol blue, a colorimetric pH indicator: (a) at the beginning of the test; (b) after 5 min and (c) after 10 min of contact between a solution containing 1 g L^{-1} of acetic acid and the acceptor solution.

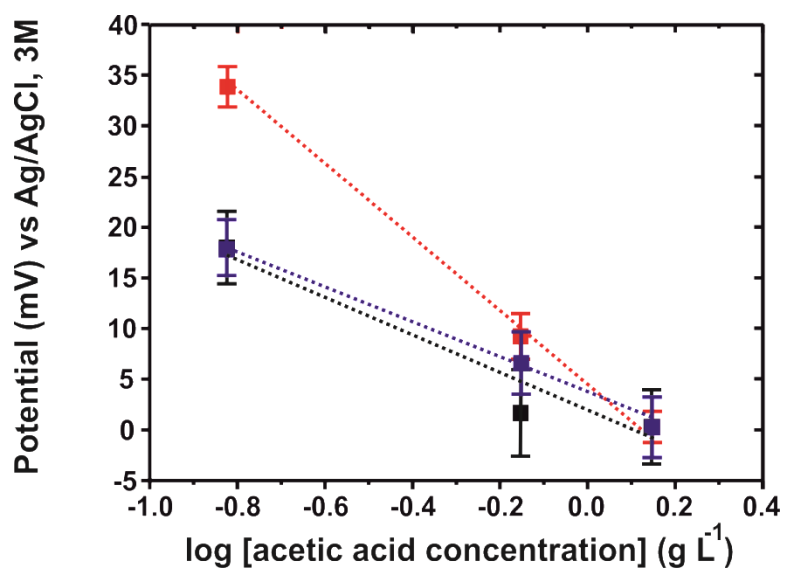


Fig. S4. Calibration curves obtained for the determination of 0.15, 0.70 and 1.40 g L⁻¹ acetic acid using an acceptor solution with 10⁻² (black color), 10⁻³ (red color) and 10⁻⁴ M (blue color) CH₃COOK concentrations. Standard deviation of triplicated calibrations in mV is drawn as error bars in the calibration plots.

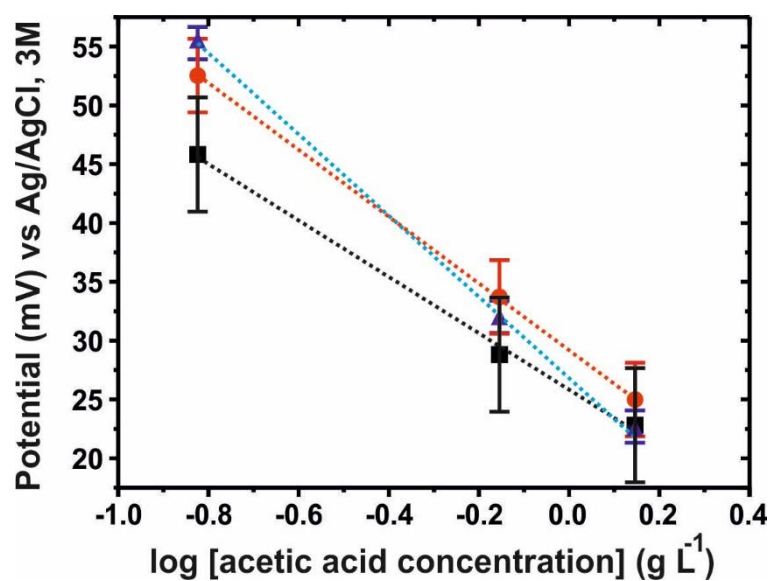


Fig. S5. Calibration curves obtained for the determination of 0.15, 0.70 and 1.4 g L⁻¹ acetic acid in presence of an acceptor solution without pH adjustment (blue color), with pH adjusted at 5.5 (black color) and with pH adjusted at 7 (red color). Standard deviation of triplicated calibrations in mV is drawn as error bars in the calibration plots.

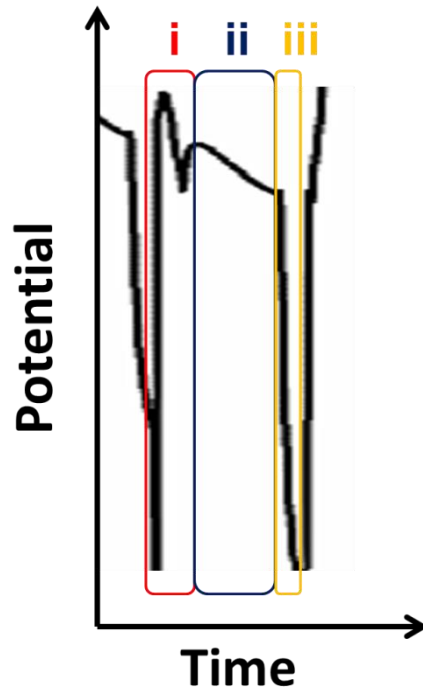


Fig. S6. Detail of one analytical response obtained during the acetic acid determination. The letters inside the plot represent the signal recorded in the three consecutive steps of the experimental procedure: (i) the acceptor and the acidified sample flowed during 5 min; (ii) the diffusion through the membrane in stop-flow during 10 min; and (iii) the signal recorded during 2 min in stop flow after flowing the acceptor solution to the pH-ISFET during 10 s.

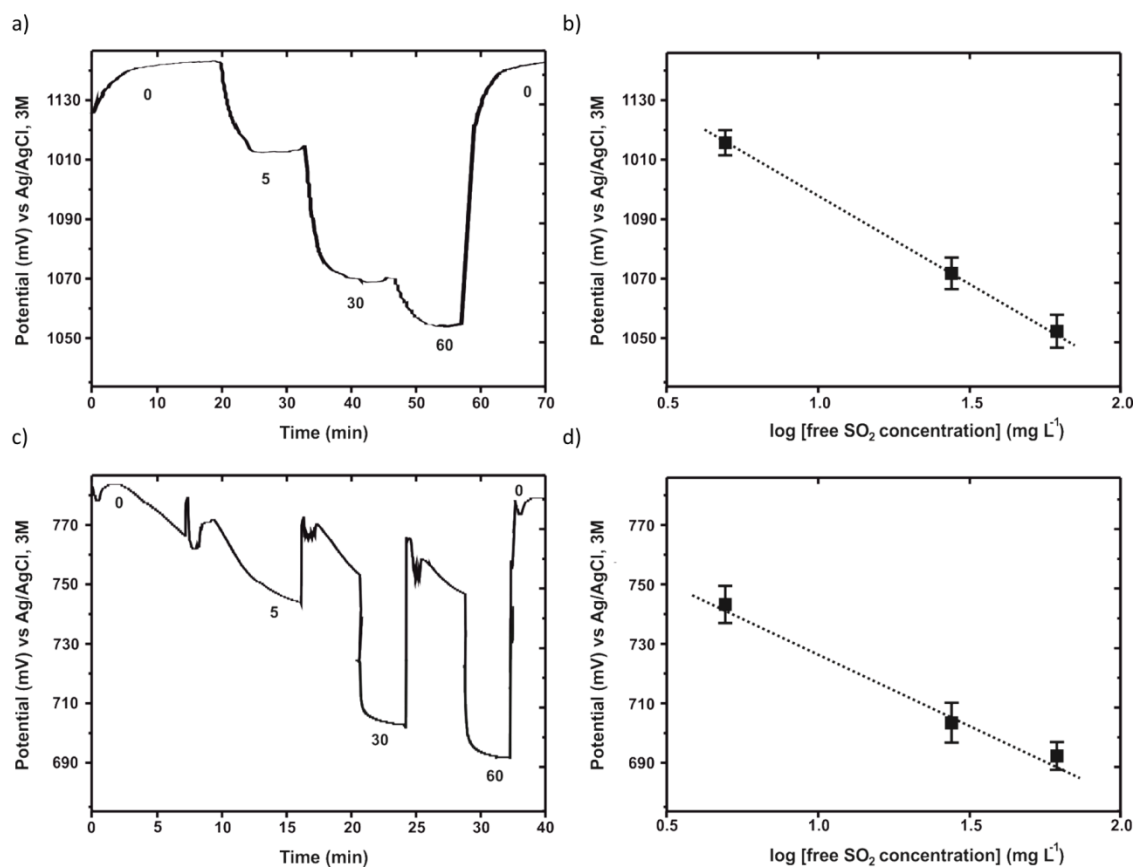


Fig. S7. a) Recording of the pH-ISFET signal (mV) under continuous flow conditions and (b) the obtained calibration plot for 0, 5, 30 and 60 mg L⁻¹ of free SO₂. c) Recording of the pH-ISFET signal (mV) under stop flow conditions and (d) the obtained calibration plot for 0, 5, 30 and 60 mg L⁻¹ of free SO₂. The numbers depicted in (a) and (c) plots represent the concentration of free SO₂ (mg L⁻¹) injected in the microanalytical flow system. Standard deviation of triplicated calibrations in mV is drawn as error bars in the calibration plots.

Table S1. Values of acetic acid concentration obtained with the microanalytical flow system for the red *Don Simón* and the white *Sumarroca* wine samples. Theoretical values correspond to the sum of the experimental value calculated from the sample without spiking acetic acid and that of each spiked sample. The standard deviation for the flow system is represented in brackets (n=3).

Wine	Acetic acid concentration (g L ⁻¹)		% Recovery*
	Flow system (n=3)	Theoretical	
<i>Don Simón</i>	0.56 (0.10)	0.56	-
<i>Don Simón</i> + 0.15 g L ⁻¹	0.67 (0.03)	0.71	94
<i>Don Simón</i> + 0.50 g L ⁻¹	1.04 (0.02)	1.06	98
<i>Don Simón</i> + 1.00 g L ⁻¹	1.56 (0.04)	1.56	100
<i>Sumarroca</i>	0.41 (0.03)	0.41	-
<i>Sumarroca</i> + 0.15 g L ⁻¹	0.54 (0.01)	0.56	96
<i>Sumarroca</i> + 0.50 g L ⁻¹	0.83 (0.05)	0.91	91
<i>Sumarroca</i> + 1.00 g L ⁻¹	1.18 (0.05)	1.41	84

* $100 \times (\text{experimental value}/\text{theoretical value})$

Table S2. Values of acetic acid concentration obtained with the microanalytical flow system and the standard method for several wine samples. The standard deviation for the microanalytical flow system (n = 3) is represented in brackets. The confidence intervals are calculated with a level of 95% for the standard method.

Wine ¹	Free acetic acid concentration (g L ⁻¹)		
	Microanalytical flow system (n=3)	Standard method ²	Relative error %
W1	0.99 (0.05)	1.20 ± 0.15	-19
W2	0.15 (0.01)	0.18 ± 0.02	-14
W3	0.18 (0.02)	0.21 ± 0.03	-16
W4	0.11 (0.01)	0.13 ± 0.02	-14
W5	0.09 (0.01)	0.12 ± 0.01	-20
R1	0.31 (0.03)	0.37 ± 0.05	-15
R2	0.45 (0.04)	0.52 ± 0.06	-14
RO1	0.18 (0.01)	0.21 ± 0.03	-15
RO2	0.15 (0.01)	0.18 ± 0.02	-16

¹W: white wine; R: red wine; RO: Rosé wine.

²Confidence interval calculated by IRTA-INCAVI from the results of inter-comparison analysis.

Table S3. Values of free SO₂ concentration obtained with the microanalytical flow system for the *Don Simón* red and the *Sumarroca* white wine samples. Theoretical values correspond to the sum of the concentration of wine calculated experimentally with the flow system plus the 70 % of added SO₂, assuming that the other 30 % is bounded to aldehydes, ketones, sugars or acids present in wines. The standard deviation for the microanalytical flow system is represented in brackets (n = 3).

Wine	Free SO ₂ concentration (mg L ⁻¹)		% Recovery
	Flow system (n=3)	Theoretical	
<i>Don Simón</i>	23 (2)	23	-
<i>Don Simón</i> + 5 mg L ⁻¹	27 (2)	27	102
<i>Don Simón</i> + 10 mg L ⁻¹	27 (2)	30	90
<i>Don Simón</i> + 15 mg L ⁻¹	31 (1)	34	91
<i>Don Simón</i> + 40 mg L ⁻¹	47 (2)	51	92
<i>Sumarroca</i>	21 (2)	21	-
<i>Sumarroca</i> + 5 mg L ⁻¹	24 (2)	25	98
<i>Sumarroca</i> + 10 mg L ⁻¹	27 (2)	28	96
<i>Sumarroca</i> + 15 mg L ⁻¹	30 (1)	32	95
<i>Sumarroca</i> + 40 mg L ⁻¹	45 (2)	49	92

Table S4. Values of free SO₂ concentration obtained with the microanalytical flow system and the standard method for several wine samples. The standard deviation for the microanalytical flow system (n = 3) is represented in brackets. The confidence intervals are calculated with a level of 95% for the standard method.

Wine ¹	Free SO ₂ concentration (mg L ⁻¹)			Volatile acidity (g L ⁻¹) ³
	Microanalytical flow system (n=3)	Standard method ²	Relative error %	
W1	15 (0)	12 ± 4	22	1.20 ± 0.15
W2	12 (0)	9 ± 3	35	0.18 ± 0.02
W3	15 (0)	12 ± 4	28	0.21 ± 0.03
W4	18 (1)	21 ± 4	-13	0.13 ± 0.02
W5	25 (2)	27 ± 8	-7	0.12 ± 0.01
R1	35 (1)	33 ± 12	5	0.37 ± 0.05
R2	16 (1)	16 ± 5	0	0.52 ± 0.06
RO1	19 (1)	23 ± 7	-18	0.21 ± 0.03
RO2	15 (0)	13 ± 4	14	0.18 ± 0.02
R1 *	36 (2)	–	10	–
W5 *	26 (2)	–	-4	–
RO2 *	15 (1)	–	15	–

¹W: white wine; R: red wine; RO: Rosé wine.

²Confidence interval calculated by IRTA-INCAVI from the results of inter-comparison analysis.

³ Standard method applied by the IRTA-INCAVI.

*Spiked with 0.7 g L⁻¹ acetic acid.

Table S5. Least squares parameters obtained comparing the microanalytical flow system and the standard method for acetic acid and free SO₂ determination. The uncertainty intervals are calculated at the 95% confidence level.

Wine*	Acetic acid		
	Slope	Intercept (g L⁻¹)	r
Red wine	0.71 ± 0.06	0.12 ± 0.03	0.98
Wine*	Free SO₂		
	Slope	Intercept (mg L⁻¹)	r
White wine	1.4 ± 0.1	-7.0 ± 3.0	0.99
Red wine	1.0 ± 0.1	0.2 ± 1.0	0.98
Rosé wine	1.0 ± 0.2	-1.0 ± 2.0	0.93

* W8 not included in the analysis of free SO₂